

Examination of Changes in Key Brain Metabolites in Faradarmangars Under the Influence of Faradarmani Consciousness Field Using Proton Magnetic Resonance Spectroscopy (^1H -MRS)

Mohammad Ali Taheri¹, Sara Torabi², Farid Semsarha^{3*}

* Corresponding author: Farid Semsarha

Email: Semsarha@ut.ac.ir

1. Sciencefact R&D Department, Cosmointel Inc.
Research Center, Ontario, Canada

2. Department of Plant Biology, School of Biology,
College of sciences, University of Tehran, Tehran, Iran

3. Institute of Biochemistry and Biophysics (IBB),
University of Tehran, Tehran, Iran

DOI: <https://doi.org/10.61450/joci.v4i19.224>

Abstract

The Faradarmani Consciousness Field is non-physical in nature. Although it cannot be quantitatively measured, its effects can be observed and examined through well-designed experiments. In this study, changes in key brain metabolites were investigated in a population of trained individuals known as Faradarmangars. In a previous study using fMRI, it was shown that certain regions of the brain were activated or deactivated under the influence of this field, while some regions remained unchanged. These specific areas were the focus of the present research. To do this, changes in the concentrations of key metabolites, including the combined NAA+NAAG, total choline, total creatine, the sum of Glu and Gln amino acids, and myo-inositol, were compared across activated, deactivated, and unaffected brain regions under two conditions: rest (without field influence) and task (with field influence). The results of this study show that most key metabolites in their total form exhibited a decreasing trend in both activated and deactivated brain regions under the influence of the Faradarmani Consciousness Field. Additionally, the correlation of changes between rest and task was initially assessed using Pearson correlation analysis. Subsequently, the overall study population was divided into two subpopulations based on the trend of changes in NAA levels—those in which NAA increased and those in which it decreased as a result of the Faradarmani treatment. Pearson correlation analysis was then repeated for the aforementioned metabolites within each subpopulation. The results indicated divergent trends between total choline and total creatine in the activation region, suggesting that these metabolites follow opposite trajectories—a pattern that may be key to the activation observed in specific brain regions among Faradarmani practitioners. The reduction in total creatine points to altered energy conditions under the influence of the Consciousness Field. A direct investigation of energy carriers using phosphorus MRS is currently planned by the authors.

Keywords: MRS spectrum, total choline, total creatine, myo-inositol, NAA, NAAG, Faradarmani

Introduction

Magnetic resonance spectroscopy (MRS) is a non-invasive technique derived from high-resolution nuclear magnetic resonance (NMR) spectroscopy (Barker and Li, 2006). While NMR has traditionally been employed to analyze the molecular structure of chemical compounds, it also laid the groundwork for applications in biological systems (Emwas et al., 2020). Building on this foundation, *in vivo* MRS was developed in the late 1970s, enabling the direct investigation of tissue metabolism and chemical composition within living organisms (Mansfield and Grannell, 1973). This advancement has proven especially valuable in neuroscience, where MRS is widely used to assess brain metabolites under both physiological and pathological conditions (Wilson et al., 2019).

In proton magnetic resonance spectroscopy (¹H-MRS) of the brain, the metabolites N-acetylaspartate (NAA), creatine (Cr), and choline (Cho) are key markers for assessing normal brain metabolism and identifying pathological changes. Changes in the relative ratios of these metabolites, such as a reduction in the NAA to creatine (NAA/Cr) ratio or an elevation in the choline to NAA (Cho/NAA) ratio, may reflect various neuropathological conditions (Weinberg et al., 2021).

The creatine (Cr) peak, resonating at approximately 3.0 parts per million (ppm), offers valuable insights into cellular energy metabolism (Verma et al., 2016). Creatine and phosphocreatine (PCr), primarily located in neurons and glial cells, play a key role in sustaining ATP levels. Therefore, alterations in the Cr peak may indicate disruptions in the brain's energy homeostasis (Dossi et al., 2019). Choline is essential to several critical biological processes, including maintaining cell membrane integrity, facilitating methylation reactions, and supporting the synthesis of key neurotransmitters. Therefore, monitoring choline peaks in MRS is a valuable tool for diagnosing brain tumors, as the rapid proliferation of cancer cells is typically associated with increased choline demand

for membrane synthesis (Yao et al., 2023). Conversely, reduced NAA levels often indicate tumor infiltration into healthy brain tissue, reflecting impaired neuronal function (Lu et al., 2024).

Glutamate (Glu) and glutamine (Gln) are among the most abundant amino acids in the human brain, with concentrations ranging from 6–13 mmol/kg and 3–6 mmol/kg of wet weight, respectively (Ramadan et al., 2013). These two compounds are metabolically interconnected, with Glu being stored as Gln in glial cells. Their balanced cycling between neurons (Glu) and glia (Gln) is crucial for normal brain function and reflects essential neuron-glia metabolic interactions. (Soto-Verdugo and Ortega, 2021). Glu also serves as the brain's primary excitatory neurotransmitter, playing a central role in synaptic activity by being released from presynaptic neurons and binding to postsynaptic receptors to trigger neuronal activation (Zhou and Danbolt, 2014).

The present study was designed to investigate a novel hypothesis grounded in the theoretical framework proposed by Taheri. According to this perspective, various T-Consciousness Fields (TCFs)—subsets of the Cosmic Consciousness Network—exist as non-physical entities. Although these fields cannot be measured using conventional quantitative tools, their effects can be examined through laboratory-based experiments. The influence of these fields is initiated through the human mind, typically by a brief moment of attention lasting only a few seconds. In this model, the brain is not regarded as the source of consciousness, but rather as a detector that receives and processes information from the mind (Taheri, 2013). This processing can lead to observable changes in brain activity. Previous studies employing EEG and fMRI techniques have reported alterations in brain function following exposure to the Faradarmani Consciousness Field, a specific type of T-Consciousness Field (Taheri et al., 2022; Taheri et al., 2022a)

It is hypothesized that when an individual initiates the use of Faradarmani through a brief moment of attention, a connection is established that allows information to be transmitted from the Faradarmani (TCF1) (Taheri et al., 2024). This informational input is proposed to influence brain function, leading to measurable changes in activity. In this study, in addition to assessing changes in key brain metabolites under the influence of the Faradarmani Consciousness Field, metabolic variations were analyzed using Pearson correlation based on the increasing or decreasing trend of NAA across the entire population as well as within subgroups.

Method

MRI was performed on a 3.0-T clinical scanner (Magnetom Prisma, Siemens Medical Solutions, Erlangen, Germany) with a gradient strength of 40 mT/m. A body-connected coil enabled the transmission of excitation. Specifically, a ^1H phased-array head coil (125 MHz) was used for signal detection (Siemens Rapid Biomedical, Germany).

After acquiring scout images of the subjects, a T2-weighted imaging protocol was performed in axial and coronal planes to capture data from the regions of interest. The MRI protocols were also followed for the MRS experiments. Data acquisition was conducted in two phases: similarly to previous steps, from baseline up to 15 minutes before the onset of treatment (rest phase), and immediately after the initiation of the treatment up to 15 minutes (task phase).

The T2-weighted imaging protocol was based on a standard spin-echo sequence with the following parameters: TR/TE = 5000/77 ms, NEX = 2, FOV = $4 \times 4 \text{ cm}^2$, matrix size = 256×256 , and slice thickness = 1 mm. Prior to performing MRS, a voxel of $1 \times 1 \times 1 \text{ cm}^3$ was defined in each of the three target regions for each subject. Following manual shimming and water suppression adjustment, short-echo proton MR spectra with high signal quality were acquired using the PRESS technique (TR/TE = 6000/135 ms, 156 acquisitions).

Before starting the MRS test, water suppression was performed using second-order shimming and a Chemical Shift Selective (CHESS) pulse sequence. At the end of the MRS experiment, the reference water signal was acquired by disabling water suppression to allow for metabolite concentration calibration. The described MRI and MRS protocols were conducted similarly both before and after the treatment process. Rest and task imaging were performed sequentially without moving the subjects and with their eyes completely closed during both phases.

Experimental design

Based on fMRI data from previous studies, in order to investigate metabolic changes in the activated and deactivated brain regions of Faradarmangars, three regions were selected: one containing an activated area (right Precentral Gyrus), one containing a deactivated area (right Superior Temporal Gyrus), and a third region with similar dimensions located between the activated and deactivated areas, which, according to the obtained data, does not show activation or deactivation in response to the Faradarmani Consciousness Field (Figure 1). The third region was chosen to serve as a negative control for comparing potential metabolic changes with the other two regions. Images of the selected regions and the MRS spectra obtained during the rest state are presented in Figures 2 to 4.

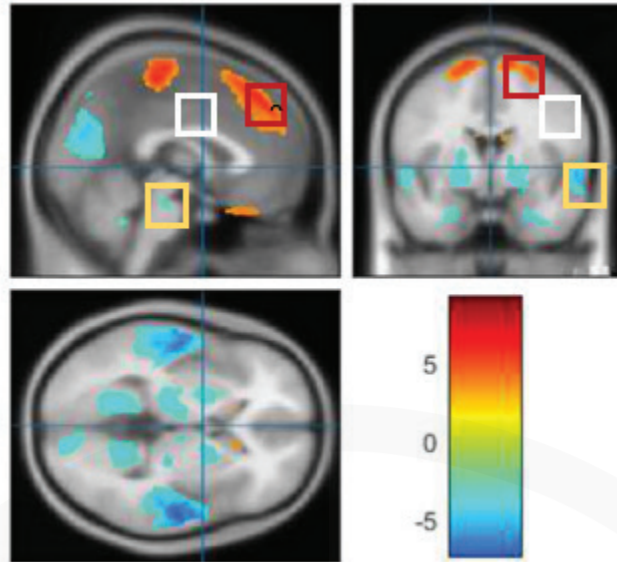


Figure 1. Three selected regions based on fMRI data. Red box: Activated region, Yellow box: Deactivated region, White box: Neither activated nor deactivated region (Taheri et al., 2022).

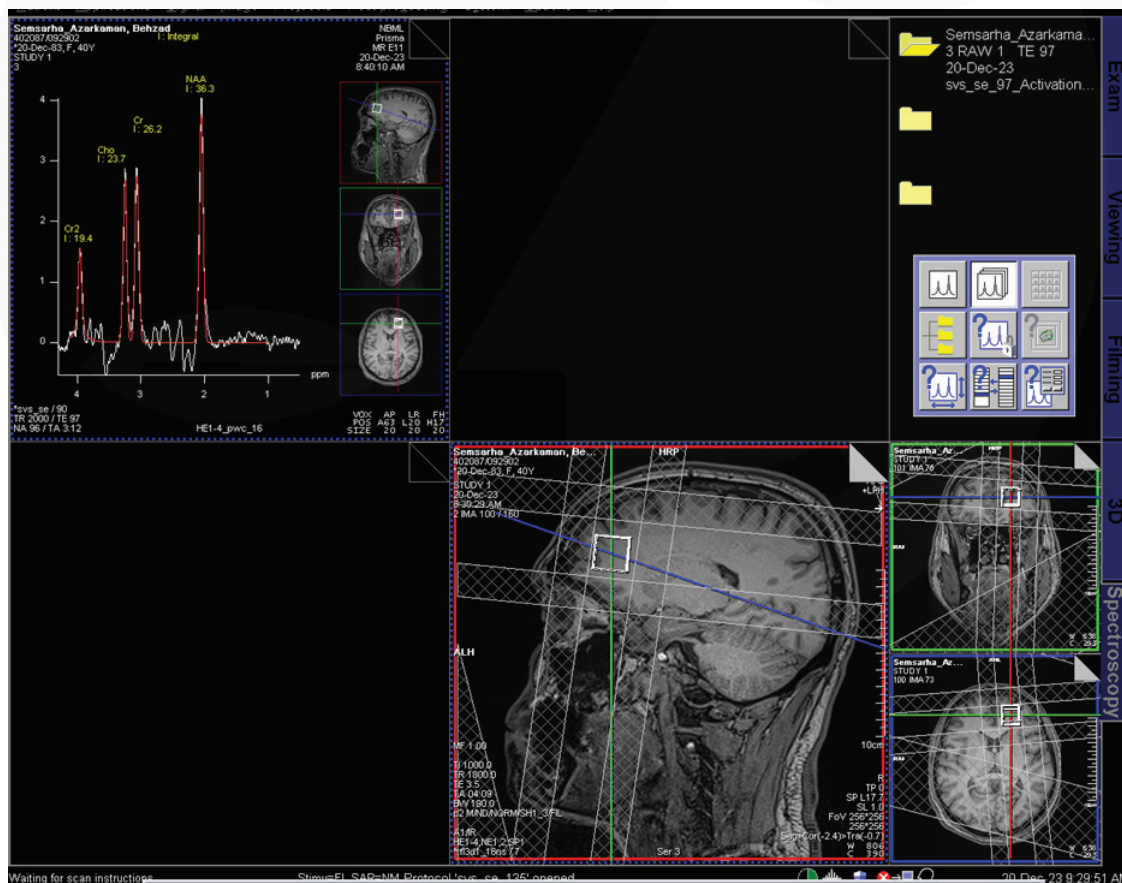


Figure 2. T2-weighted MR image of one of the study subjects, showing the placement of the MRS voxel on the selected activated region under Faradarmani Consciousness Field treatment, along with the proton spectrum obtained in the rest state.

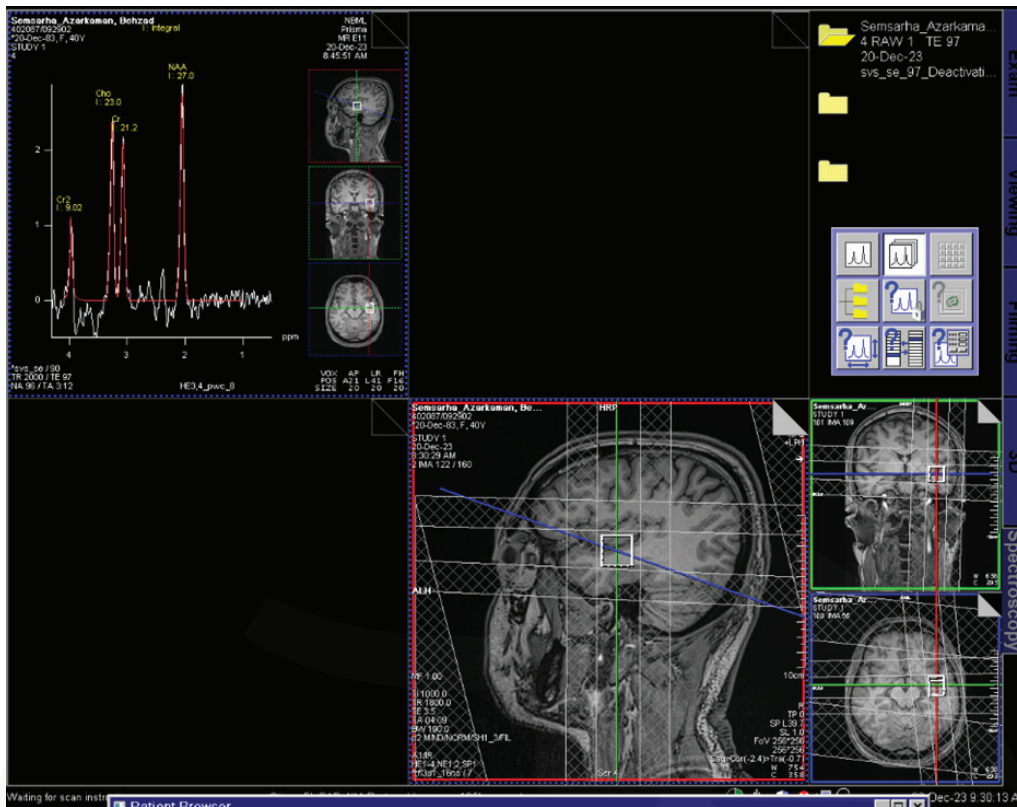


Figure 3. T2-weighted MR image of one of the study subjects, showing the placement of the MRS voxel on the selected deactivated region under Faradarmani Consciousness Field treatment, along with the proton spectrum obtained in the rest state.

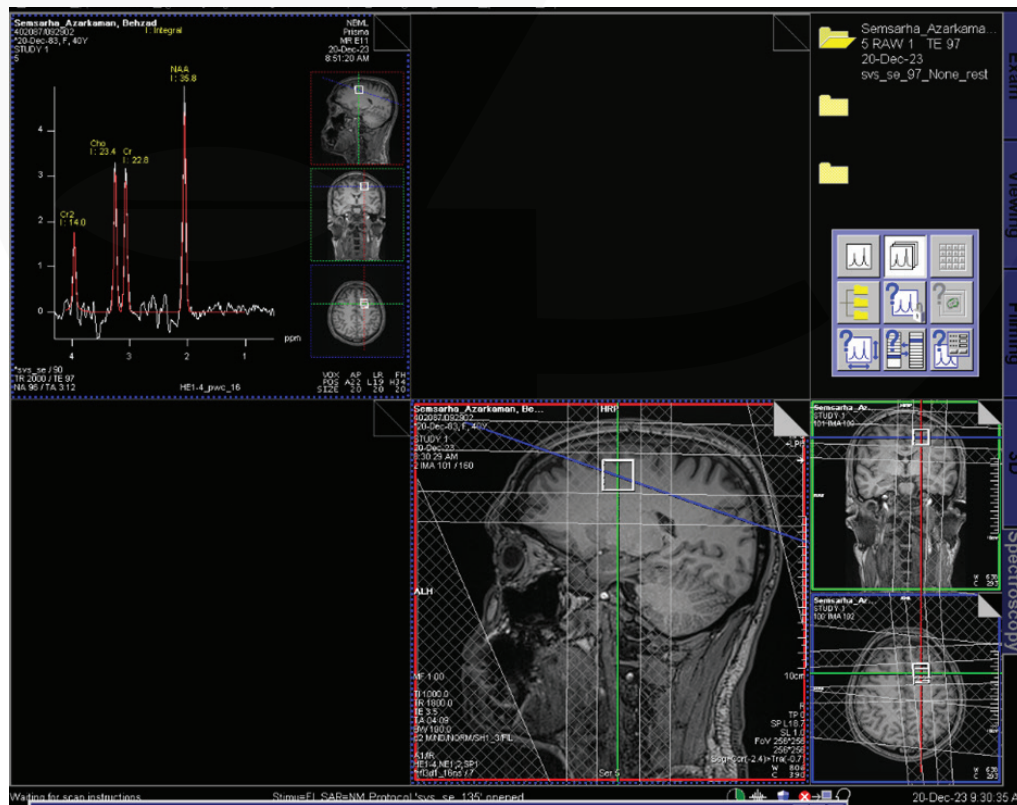


Figure 4. T2-weighted MR image of one of the study subjects, showing the placement of the MRS voxel on the selected neither activated nor deactivated region during Faradarmani Consciousness Field treatment, along with the proton spectrum obtained in the rest state.

Analysis of the MR spectrum

The volume of interest (VOI) for the MRS experiments was drawn on T2-weighted images. We attempted to create identical VOIs for the three regions across different subjects to ensure similar coverage of the target areas in each individual. Each spectrum corresponding to the selected regions was analyzed using a Java-based graphical user interface. This interface, used for the MRUI quantification package, contains a basic knowledge base of 57 peaks associated with at least 34 different metabolites. Metabolite concentrations were determined relative to the water signal used as a reference. Therefore, all amplitudes in each MR spectrum were expressed semi-quantitatively. It is also worth mentioning that the advanced method for accurate, robust, and efficient spectral fitting (AMARES) was used for quantification (Vanhamme et al., 1997).

The Application of Faradarmani Consciousness Field

In the present study, a population-level MRS analysis was conducted on Faradarmangars, comparing metabolite changes in selected brain regions during the task and rest phases. The task refers to the activity during which a Faradarmangar personally connects to the Cosmic Consciousness Network. This study was approved by the Ethics Committee of Iran University of Medical Sciences (Approval ID: IR.IUMS.REC.1402.940).

Thirty healthy adult participants (mean age: 42 ± 7 years), all with no history of neurological or psychiatric medication use in the six months prior to the test day, were included in the study group. Of these participants, 40% were male ($n = 12$) and 60% were female ($n = 18$). The design of the studies conducted using the MRS technique included a 15-minute rest phase (prior to connection with the field) and a 15-minute task phase, representing the state of connection with the Faradarmani Consciousness Field (initiated immediately after the rest phase).

Further details about each phase of the study in chronological order are as follows:

1. **Rest:** A 15-minute initial phase in which Faradarmangars were instructed, while inside the MRI scanner, to keep their eyes closed and remain relaxed and stress-free, without engaging with any Consciousness Fields. The purpose of this phase was to obtain control data, representing the baseline state before connection with the field. This baseline plays a critical role in constructing population-level control data or "pre-connection" references.
2. **Task:** In this study, the second 15-minute phase—immediately following the rest phase without any temporal gap—is referred to as the task phase. In this phase, the individuals establish a connection with the Faradarmani Consciousness Field. This connection is initiated solely by the participants themselves upon hearing a predefined beep, which they had been informed in advance signals the beginning of the connection.

Data Analysis

The data obtained from this study were statistically analyzed using GraphPad Prism software (version 9). One-way analysis of variance (ANOVA) was used to assess differences in metabolite levels between the rest and task phases. For each group's MRS dataset, the Wilcoxon test was applied at a 5% significance level to compare changes in metabolite concentrations between these two phases. Pearson correlation analysis and the calculation of correlation coefficients (r) were conducted using a two-tailed p -value. A p -value of less than 0.05 was considered statistically significant.

Results and Discussion

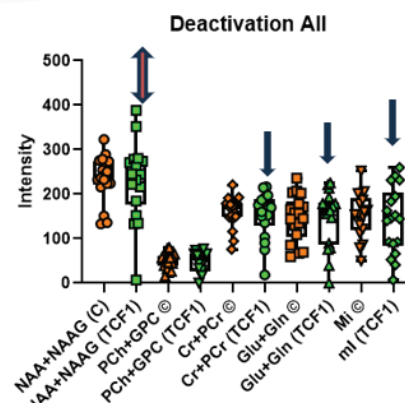
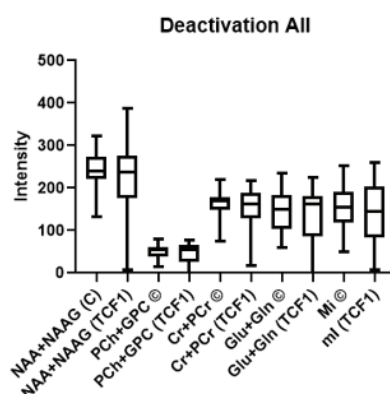
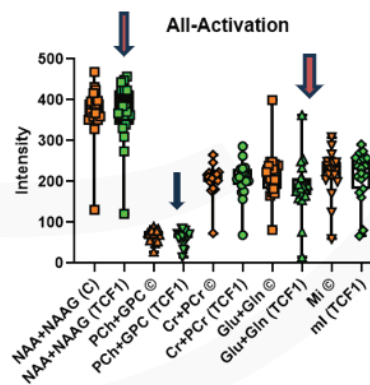
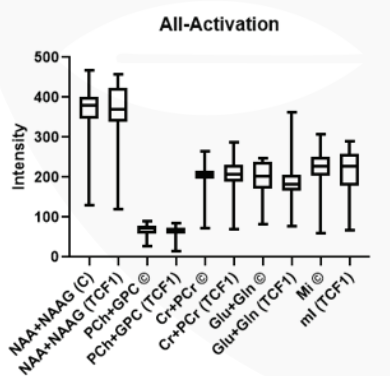
Figure 5 shows the changes in key MRS peak metabolites under rest and task conditions. It can be observed that in the activation region, a decreasing trend in total NAA, total choline,

glutamine, and glutamic acid was recorded under the influence of the Faradarmani Consciousness Field. In the deactivation region, as shown in the box plot, NAA levels during the task condition exhibited an increasing trend compared to the maximum threshold at rest, while also showing a decrease relative to the minimum threshold at rest. However, other metabolites—total creatine, myo-inositol, glutamine, and glutamic acid—displayed a downward trend during the task condition. In the 'None' region—defined as the brain area that showed no measurable change under the influence of the Faradarmani Consciousness Field—similar trends were observed between rest and task conditions, with only minor variations reflected in the median values of the box plot.

Under typical conditions, increased brain activity is accompanied by elevated turnover of key brain metabolites such as N-acetylaspartate, which reflects neuronal integrity and mitochondrial function (Paslakis et al., 2014); choline, which is involved in membrane synthesis and turnover; and glutamate, the brain's primary excitatory neurotransmitter

(Wolinsky and Narayana, 2002). However, the reduction in these metabolites despite fMRI activation suggests that the brain may not be relying solely on conventional metabolic pathways. This observation aligns with Taheri's hypothesis of biological dark energy, which proposes the existence of an alternative energy source capable of supporting cellular and neural functions independently of conventional ATP production. Further experiments, especially those measuring real-time ATP production, mitochondrial function, and phosphorus-based MRS, are needed to validate this alternative energy hypothesis

The mean normalized values of metabolite changes are also presented in Table 1 and Figure 6. Similar values can be observed in the 'None' region during both rest and task conditions. In the activation region, these values are comparable to those in the 'None' region and, in some cases, even lower. In contrast, a clear decreasing trend is evident in the deactivation region when compared to the other areas.



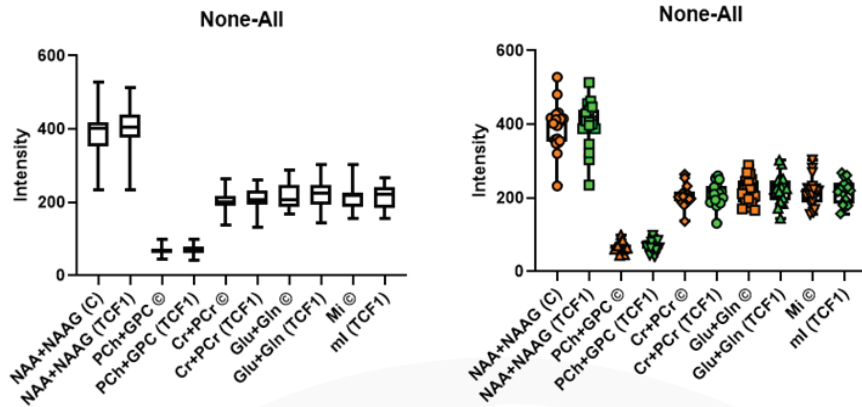


Figure 5. Comparison of changes in key metabolite levels across three different brain regions in Faradarmangars: top – activation region; middle – deactivation region; bottom – None region. C: rest; task: TCF1. (The left and right figures both illustrate metabolite changes, and the data distribution is presented in two formats to allow a clearer observation of the trends in variation.)

Table 1. The changes in the mean normalized values of key metabolomes across different brain regions in Faradarmangars. (c): rest or control; (TCF1): task condition.

	NAA+NAAG (C)	NAA+NAAG (TCF1)	PCh+GPC ©	PCh+GPC (TCF1)	Cr+PCr ©	Cr+PCr (TCF1)	Glu+Gln ©	Glu+Gln (TCF1)	Mi ©	ml (TCF1)
Ave-Activation	370.58	369.11	67.12	62.39	204.19	205.43	220.41	185.91	221.51	215.08
SD	68.78189909	77.58	14.61	18.71	37.72	44.53	87.35	69.61	56.66	60.65
Ave-Deactivation	235.2521667	228.0478333	50.535	47.70183333	160.1137	151.8888	145.7506	145.6489	152.2921	140.4383
SD	51.47	86.23	17.44	22.89	35.51	51.31	51.84	63.22	50.29	74.68
Ave-None	391.85	397.32	68.11	67.95	204.35	209.30	217.54	222.36	216.70	217.07
SD	63.80	64.21	13.22	13.63	28.14	30.58	36.95	39.31	39.42	32.15

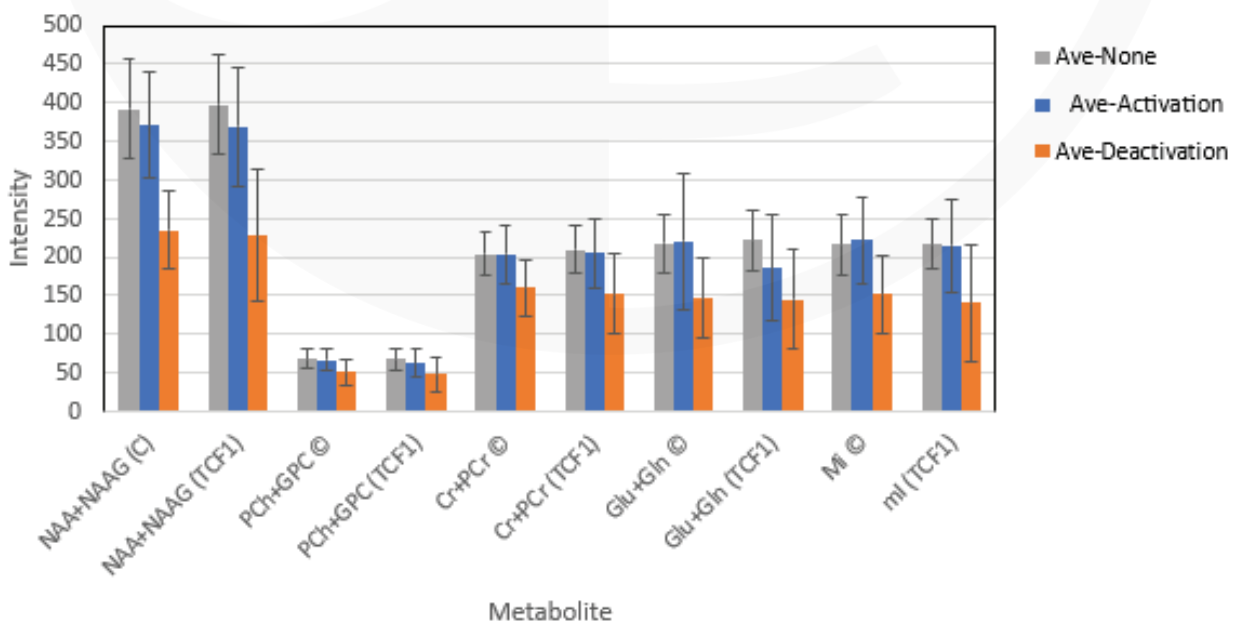


Figure 6. Bar chart showing changes in metabolite levels by subpopulation. C: rest; TCF1: task or under the influence of Faradarmani Consciousness Field.

According to the obtained data, the levels of key metabolites in the deactivation region are generally lower than those in the activation and None regions of the Faradarmangars' brain. This difference becomes more pronounced under the influence of the Faradarmani Consciousness Field or during the task condition, compared to the rest or baseline condition (Figure 6).

To gain a deeper understanding of the changes in key metabolites during the task condition, Pearson correlation analysis was performed, and correlation coefficients (r) were calculated. This analysis yields a score ranging from +1 to -1. A score of +1

indicates a strong positive correlation, meaning the two variables change in a similar manner. A score near zero suggests no correlation, while a score near -1 indicates a strong negative correlation, meaning the variables change in opposite directions. The Pearson correlation coefficient (r) for two paired-variable objects sums the product of their differences from their respective means and divides this total by the product of the square roots of the squared differences from their means. In Figure 7, the Pearson correlation of changes in key metabolite levels under rest and task conditions is presented for the overall population.

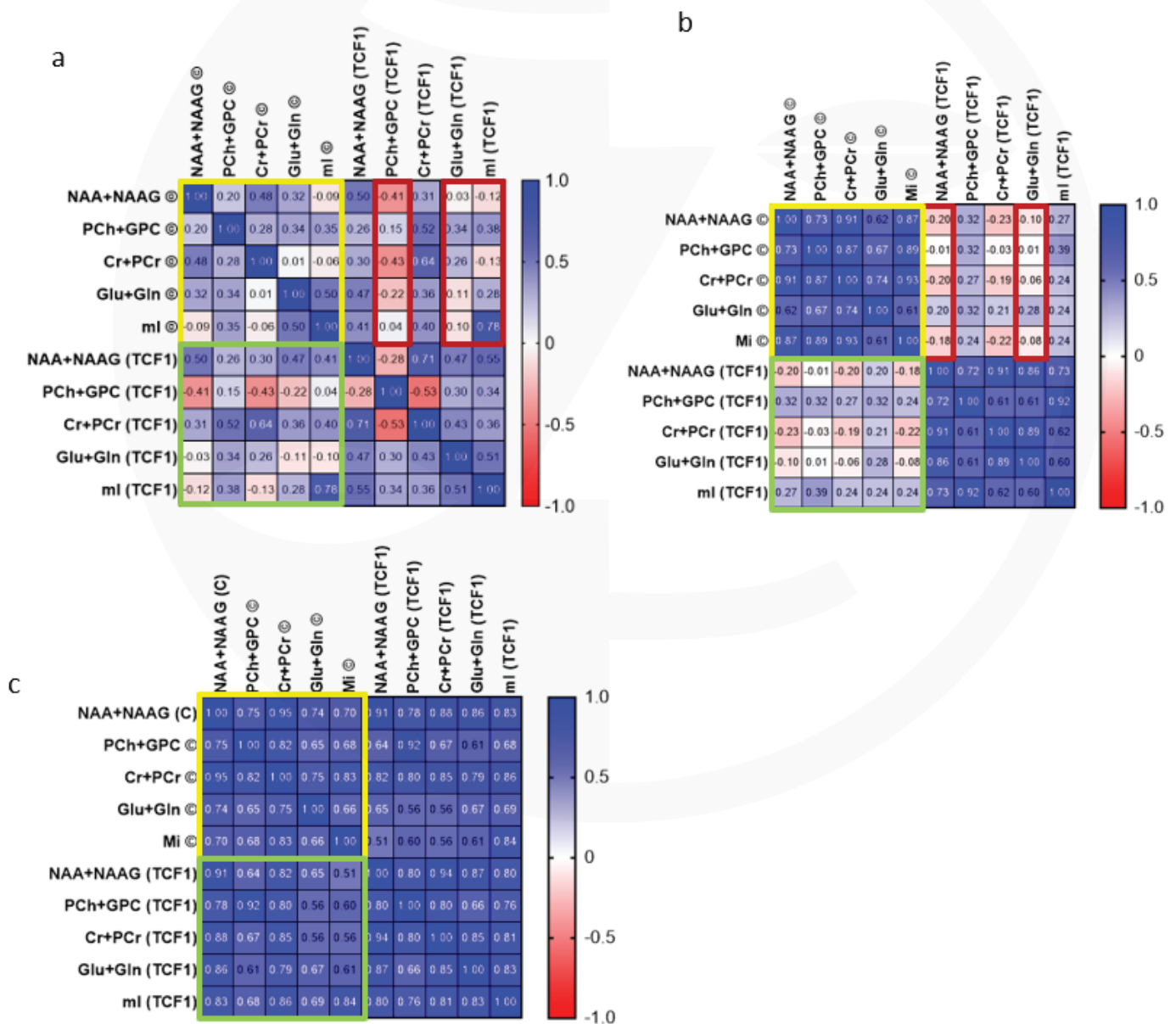


Figure 7. Correlation analysis of changes in key metabolites in the overall population. a: Activation region; b: Deactivation region, and c: None.

As shown in Figure 7, in the deactivation region of the brain under the influence of the Faradarmani Consciousness Field, the correlation of metabolite changes shifts from values above zero—seen in comparisons of rest-rest and task-task conditions—to values near zero or negative when comparing rest and task conditions. This shift is distinctly different from the patterns observed in the other two brain regions. In the 'None' region, the figure clearly shows consistently positive correlations across all sample comparisons. In the activation region, a different pattern of metabolite changes is observed in the Pearson correlation analysis. Specifically, the changes in total choline during the task condition show a tendency toward negative or near-zero values when compared to other metabolites in the rest condition—particularly for myo-inositol. Moreover, in

the task-task comparison, an inverse trend is observed between total creatine and total choline, whereas these two metabolites showed a direct correlation in the rest samples.

In the continuation of this study and to conduct a more detailed and precise analysis of the correlations between metabolite changes in different brain regions, the overall population was divided based on the change in NAA levels—the most abundant and prominent brain metabolite in MRS analyses. The participants were categorized into two subpopulations: one showing an increase in NAA as a result of the Faradarmani treatment (NAA+) and the other showing a decrease in NAA due to the treatment (NAA-). Pearson correlation analysis was then performed separately within these subpopulations (Figure 8).

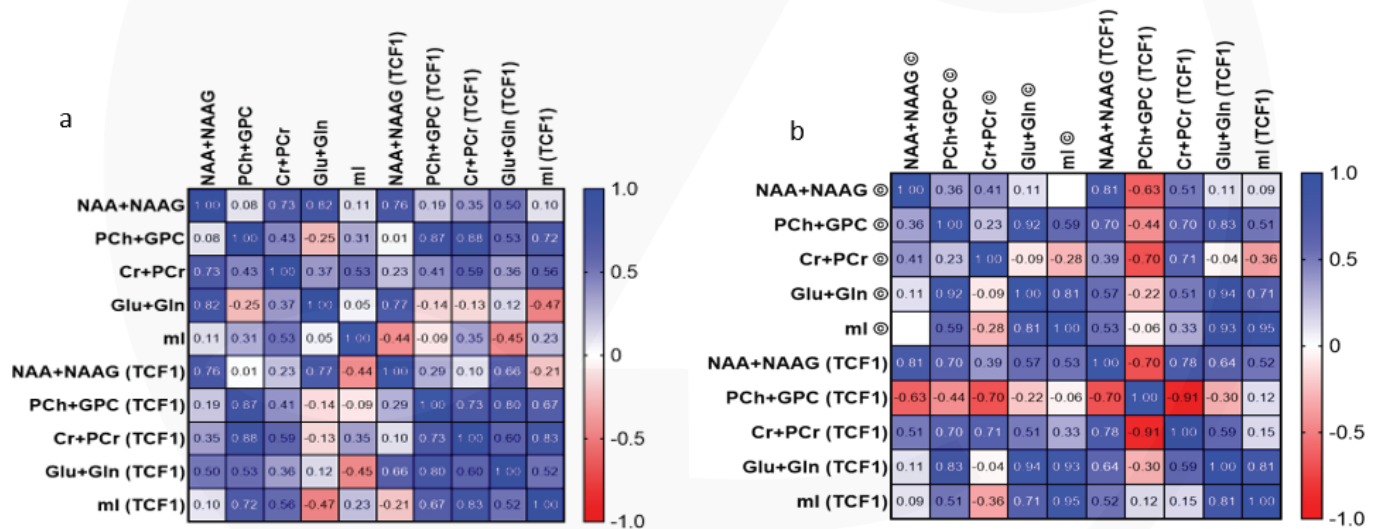


Figure 8. Correlation analysis of changes in key metabolites in the two subpopulations of this study within the brain activation region under the influence of Faradarmani Consciousness Field. a: NAA+; b: NAA-

Figure 8 illustrates the changes in metabolites across the two subpopulations. The most notable change is observed in the NAA- group, where an increase in total choline is evident, while other metabolites, particularly total creatine, show a decreasing trend. The divergent changes in total choline and total creatine in the activation region suggest that the opposing dynamics of these metabolites may play a key role in the activation of brain areas observed in Faradarmangars.

Referring to the data presented in the first study of this issue, it becomes clear that this change is particularly prominent in the brains of male Faradarmangars, where, in contrast to the female population, greater activation was observed.

As mentioned in the introduction, creatine plays a central role in maintaining cellular ATP levels. In Figure 7b, a reduction in total creatine is observed during the task condition within the

deactivation region. This reduction may reflect an adaptive energy redistribution strategy, where metabolic demand is downregulated in task-negative areas to support more efficient functioning in task-positive networks. Similar to the typical deactivation pattern of the default mode network (DMN) during cognitive engagement (Anticevic et al., 2012), the negative correlation between rest and task conditions could represent a compensatory response to energy demands. Paradoxically, however, our EEG data revealed increased activity in BA31 (posterior cingulate cortex), a key DMN hub, under the influence of the Faradarmani Consciousness Field, contrary to the DMN suppression usually

reported in externally focused cognitive tasks (Taheri et al., 2022).

Additionally, in the activation region, a subpopulation with decreasing NAA levels (NAA-) showed a corresponding decline in total creatine during the task condition, further indicating a shift in energy dynamics (Figure 8). These observations suggest that an alternative energetic mechanism may be engaged under Faradarmani. As mentioned above, this observation aligns with the concept of biological dark energy introduced by Taheri and warrants further investigation.

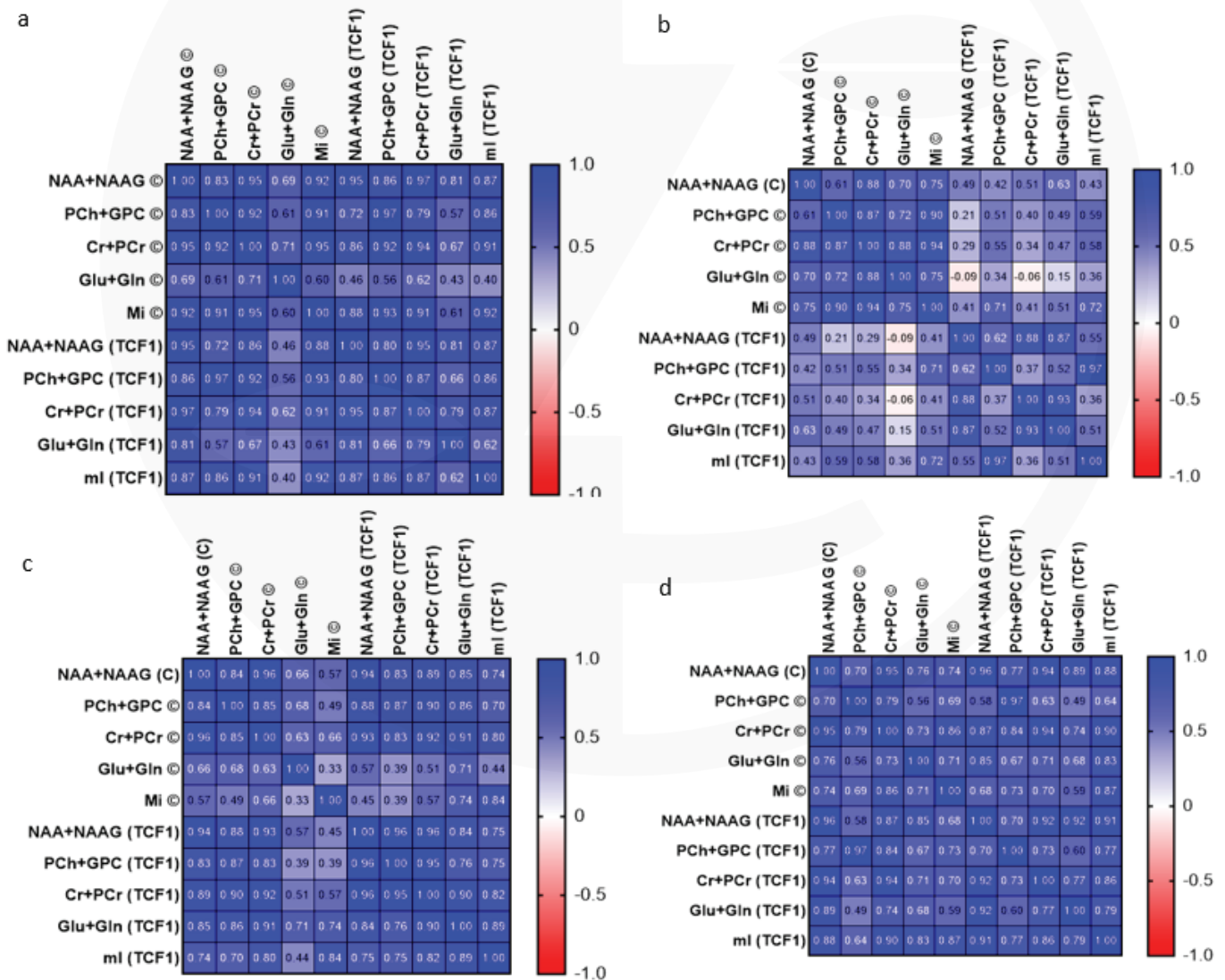


Figure 9. Correlation analysis of changes in key metabolites in the two subpopulations within the deactivation and None regions of Faradarmangars' brains. a: Deactivation NAA+, b: Deactivation NAA-, c: None NAA+, d: None NAA-

The Pearson correlation analysis of changes in key metabolites in the overall population, without division into subpopulations, primarily indicates a distinct difference in metabolic behavior between the activation and deactivation regions compared to the None region. This supports the influence of the Faradarmani Consciousness Field observed in the fMRI data. In fact, in the region where no effect of Faradarmani was detected at the brain level in the fMRI data (the None region), no corresponding metabolic changes were observed either. Secondly, the data reveal a significant and notable difference between the deactivation and activation regions. Clear and well-defined metabolic changes are observed in the deactivation region when comparing rest and task conditions. This observation aligns with the fMRI data, which also highlights the deactivation regions as more prominent in terms of the number of affected areas and the intensity of changes compared to the activation regions.

Although the Faradarmani Consciousness Field led to an increase in amino acid markers (Gln and Glu) in the deactivation region, it caused a significant rise in total choline in the activation region. The rise in glutamine (Gln) and glutamic acid (Glu) suggests enhanced glutamatergic turnover. According to Tani et al. (2014), synthesized Gln is transferred to presynaptic neurons, where it serves as the precursor for synaptic Glu; together, these processes form the glutamine–glutamate cycle (Tani et al., 2014). This observation indicates that a downregulation in neural activity does not necessarily imply metabolic inactivity. Instead, it may reflect a shift toward more efficient or reorganized neural processing, in which amino acid cycling and neurotransmitter regulation play key roles.

Overall, building on previous findings, the current study not only provides further evidence of Faradarmani's effects on brain activity but also investigates how such non-physical informational input may alter the dynamics of brain metabolomes.

References

- Anticevic, A., Cole, M. W., Murray, J. D., Corlett, P. R., Wang, X. J., & Krystal, J. H. (2012). The role of default network deactivation in cognition and disease. *Trends in cognitive sciences*, 16(12), 584–592. <https://doi.org/10.1016/j.tics.2012.10.008>
- Barker, P. B., & Lin, D. D. M. (2006). In vivo proton MR spectroscopy of the human brain. *Progress in Nuclear Magnetic Resonance Spectroscopy*, 49(2), 99-128. <https://doi.org/10.1016/j.pnmrs.2006.06.002>
- Dossi, G., Squarcina, L., & Rango, M. (2019). In Vivo Mitochondrial Function in Idiopathic and Genetic Parkinson's Disease. *Metabolites*, 10(1), 19. <https://doi.org/10.3390/metabo10010019>
- Emwas, A. H., Szczepski, K., Poulson, B. G., Chandra, K., McKay, R. T., Dhahri, M., Alahmari, F., Jaremko, L., Lachowicz, J. I., & Jaremko, M. (2020). NMR as a "Gold Standard" Method in Drug Design and Discovery. *Molecules (Basel, Switzerland)*, 25(20), 4597. <https://doi.org/10.3390/molecules25204597>
- Lu, W., Feng, J., Zou, Y., Liu, Y., Gao, P., Zhao, Y., Wu, X., & Ma, H. (2024). 1H-MRS parameters in non-enhancing peritumoral regions can predict the recurrence of glioblastoma. *Scientific reports*, 14(1), 29258. <https://doi.org/10.1038/s41598-024-80610-z>
- Mansfield, P., & Grannell, P. K. (1973). NMR'diffraction'in solids?. *Journal of Physics C: solid state physics*, 6(22), L422.DOI: 10.1088/0022-3719/6/22/007
- Paslakis, G., Träber, F., Roberz, J., Block, W., & Jessen, F. (2014). N-acetyl-aspartate (NAA) as a correlate of pharmacological treatment in psychiatric disorders: a systematic review. *European neuropsychopharmacology : the journal of the European College of Neuropsychopharmacology*, 24(10), 1659–1675. <https://doi.org/10.1016/j.euroneuro.2014.06.004>
- Ramadan, S., Lin, A., & Stanwell, P. (2013). Glutamate and glutamine: a review of in vivo MRS in the human brain. *NMR in biomedicine*, 26(12), 1630–1646. <https://doi.org/10.1002/nbm.3045>
- Soto-Verdugo, J., & Ortega, A. (2021). Critical Involvement of Glial Cells in Manganese Neurotoxicity. *BioMed research international*, 2021, 1596185. <https://doi.org/10.1155/2021/1596185>
- Taheri MA. (2013). Human from another outlook. Interuniversal Press. 2nd Edition. ISBN-13: 978-1939507006, ISBN-10: 1939507006 2013.
- Taheri, M. A., Modarresi-Asem, F., & Semsarha, F. (2022). An Investigation of the Electrical Activity of the Brain during the Treatment with Faradarmani Consciousness Field in the Faradarmangar Population. *The Scientific Journal of Cosmointel*, 1(2), 22–32. <https://doi.org/10.61450/joci.v1i2.19>
- Taheri, M. A., Torabi, S., A. Elmetwally, M., & Semsarha, F. (2024). Effects of T-Consciousness Fields on Mouse Oocyte Maturation and Embryo Development Following IVF. *The Scientific Journal of Cosmointel*, 3(15), 11–24. <https://doi.org/10.61450/joci.v3i15.195>
- Taheri, M. A., Torabi, S., Nabavi, N., Modarresi-Asem, F., Abbasi Sisara, M., Maftoun, P., & Semsarha, F. (2022a). Task-fMRI Group and Functional Connectivity Analysis of the Brain During Faradarmani Consciousness Field Connection. *The Scientific Journal of Cosmointel*, 1(2), 46–55. <https://doi.org/10.61450/joci.v1i2.19>

org/10.61450/joci.v1i2.29

Tani, H., Dulla, C. G., Farzampour, Z., Taylor-Weiner, A., Huguenard, J. R., & Reimer, R. J. (2014). A local glutamate-glutamine cycle sustains synaptic excitatory transmitter release. *Neuron*, *81*(4), 888–900. <https://doi.org/10.1016/j.neuron.2013.12.026>

Vanhamme, L., van den Boogaart A, & Van Huffel S (1997). Improved method for accurate and efficient quantification of MRS data with use of prior knowledge. *Journal of magnetic resonance (San Diego, Calif. : 1997)*, *129*(1), 35–43. <https://doi.org/10.1006/jmre.1997.1244>

Verma, A., Kumar, I., Verma, N., Aggarwal, P., & Ojha, R. (2016). Magnetic resonance spectroscopy - Revisiting the biochemical and molecular milieu of brain tumors. *BBA clinical*, *5*, 170–178. <https://doi.org/10.1016/j.bbacli.2016.04.002>

Weinberg, B. D., Kuruva, M., Shim, H., & Mullins, M. E. (2021). Clinical Applications of Magnetic Resonance Spectroscopy in Brain Tumors: From Diagnosis to Treatment. *Radiologic clinics of North America*, *59*(3), 349–362. <https://doi.org/10.1016/j.rcl.2021.01.004>

Wilson, M., Andronesi, O., Barker, P. B., Bartha, R., Bizzi, A., Bolan, P. J., ... & Howe, F. A. (2019). Methodological consensus on clinical proton MRS of the brain: Review and recommendations. *Magnetic resonance in medicine*, *82*(2), 527-550. <https://doi.org/10.1002/mrm.27742>

Wolinsky, J. S., & Narayana, P. A. (2002). Magnetic resonance spectroscopy in multiple sclerosis: window into the diseased brain. *Current opinion in neurology*, *15*(3), 247–251. <https://doi.org/10.1097/00019052-200206000-00004>

Yao, N., Li, W., Xu, G., Duan, N., Yu, G., & Qu, J. (2023). Choline metabolism and its implications in cancer. *Frontiers in oncology*, *13*, 1234887. <https://doi.org/10.3389/fonc.2023.1234887>

Zhou, Y., & Danbolt, N. C. (2014). Glutamate as a neurotransmitter in the healthy brain. *Journal of neural transmission (Vienna, Austria : 1996)*, *121*(8), 799–817. <https://doi.org/10.1007/s00702-014-1180-8>